

# Optimizing object-based image analysis for semi-automated geomorphological mapping

Niels Anders, Harry Seijmonsbergen, Willem Bouten  
 Institute of Biodiversity of Ecosystem Dynamics  
 University of Amsterdam  
 Amsterdam, The Netherlands  
 n.s.anders@uva.nl

Mike Smith  
 Centre for Earth and Environmental Science Research  
 Kingston University London  
 Kingston on Thames, United Kingdom  
 michael.smith@kingston.ac.uk

**Abstract**—Object-Based Image Analysis (OBIA) is considered a useful tool for analyzing high-resolution digital terrain data. In the past, both segmentation and classification parameters were optimized manually by trial and error. We propose a method to automatically optimize classification parameters for increasing the accuracy and efficiency of OBIA for semi-automated geomorphological mapping. We test our method by semi-automatically extracting three geomorphological ‘feature types’ (river terrace, gypsum sink holes, and fluvial incision) from a 1m Digital Terrain Model (DTM) of an alpine area in Vorarlberg, Austria. Segmentation parameters were optimized for each specific geomorphological ‘feature type’, by comparing frequency distribution matrices of training samples and automatically generated image objects. Subsequently image objects are iteratively classified with varying classification settings. The best classification scores and corresponding segmentation and classification settings are summarized in a library of feature signatures for stratified feature extraction. Our results show that through optimization, a limited number of classifiers can be used to accurately classify geomorphological features in complex terrain. This allows classification schemes to be standardized for automated and effective analysis of high-resolution terrain data. In addition, by automating mapping procedures, this research increases the efficiency of geomorphological research. Further research will include the classification of the remaining geomorphological ‘feature types’ to create a full-covered geomorphological map, and the application of the feature signature library to other areas.

## I. INTRODUCTION

Recent developments in data acquisition technology have led to the wide availability of high-resolution digital terrain data. New data analysis techniques are therefore necessary to effectively analyze this type of data in order to increase efficiency, detail and accuracy in geomorphological research. Object-Based Image Analysis (OBIA) has become an acknowledged tool for analyzing such high-resolution datasets [1, 5]. OBIA first clusters grid cells into image objects (i.e. image

segmentation), after which these objects are classified based on user-specified classification rules (see Fig. 1). Until recently image segmentation and classification settings were optimized based on time-consuming heuristics.

Anders et al. [1] recently developed a new method to optimize segmentation parameters for accurate delineation of specific geomorphological features. By using a stratified image segmentation and feature classification approach they were able to semi-automatically map alpine geomorphology in high spatial detail with an average accuracy of 71%.

Here we propose a method to automate the optimization of the classification rules (Fig. 1). We apply a segmentation accuracy assessment to determine best segmentation parameters, which are used to create image objects of specific geomorphological ‘feature types’, based on the segmentation algorithm of [2]. The classification rules are then optimized by iteratively assessing classification results with varying classification settings. We illustrate the approach by automatically extracting three contrasting geomorphological ‘feature types’ in a complex mountain landscape.

## II. METHODS

### A. Study area

The method was tested in an alpine catchment (10 km<sup>2</sup>) near the municipality of Nenzing, in the Province of Vorarlberg in western Austria, which is drained by the river Gamp. The area is mainly underlain by limestone and dolomite formations, and is characterized by gypsum karst. Glacially eroded bedrock slopes have been subject to post-glacial activity. Current geomorphological processes include mechanical weathering, debris flows, rock fall, fluvial erosion and gypsum karst [4]. The complexity of the environment makes this a challenging test area for the semi-automated classification of geomorphological features. We demonstrate our method by extracting three geomorphological

‘feature types’ that differ in their morphology, size and genesis, i.e. ‘river terrace’, ‘gypsum sink holes’, and ‘fluvial incision by the river Gamp’.

**B. LiDAR data**

LiDAR data was acquired in 2004 with an ALTM 2050 scanner. After filtering the ground points from non-ground points, a 1 m DTM was created using linear least squares interpolation. The data acquisition, filtering, and DTM processing were conducted by the company TopScan.

**C. Calculating Land-Surface Parameters**

We selected several Land-Surface Parameters (LSPs) that we considered valuable for geomorphological processes, the delineation of geomorphological features by image segmentation, and the classification of the aforementioned geomorphological ‘feature types,’ namely: slope angle, topographic openness [6], relative elevation, and upstream area (using a hydrologically conditioned DTM). We calculated openness over a radius of 25m (TO25) and 250m (TO250) to represent topographic variation at a small (within individual features) and large scale (beyond individual features). Also relative elevation was calculated over a 250m radius (REL250) to represent the relative position of features in the landscape. Moreover, we calculated the difference between the original DTM and the conditioned DTM to calculate the ‘filled area’ to highlight local depressions.

**D. Creating reference material**

The slope, TO25 and TO250 LSPs were combined into a single RGB composite (Fig. 2A-B) for creating reference material. In order to assess segmentation accuracy, we manually digitized three training samples per geomorphological ‘feature type’ (Fig. 2A) to compare with automatically generated image objects (Fig. 2B). Point-based reference data were collected to assess classification accuracy. The training samples and point data were collected based on interpretation of the RGB composite, and were visually compared with a 1:10,000 field map of [4] to ensure their accuracy.

**E. Segmentation parametrization**

Following Anders et al. [1], we used training samples to calculate characteristic 2D frequency distribution matrices of slope and TO250 values of specific geomorphological ‘feature types’ (Fig. 2C). Both slope and TO250 were selected as criteria, because slope is a key parameter for geomorphological processes and TO250 clearly visualizes feature boundaries. Subsequently, image objects were created with scale parameter values ranging from 1 – 1000. Then the frequency distribution matrices of the training samples were compared to the matrices of automatically generated image objects, see Fig. 2D. The difference between frequency distribution values of training samples and image objects were calculated as a normalized error ( $e$ ), see Fig. 2E:

$$e = \frac{H_f}{m} - \frac{H_o}{n} \tag{1}$$

where  $H_f$  and  $H_o$  are the frequency distribution values of a specific training sample and corresponding image object, respectively, and  $m$  and  $n$  are the number of grid cells captured within the training sample or object. Subsequently the sum of absolute error was calculated to summarize the total error of the image object with respect to the training sample:

$$SAE = \sum_{i=1}^k |e_i| \tag{2}$$

where  $k$  is the number of bins (i.e. 30x30). The mean SAE of the three training samples was used to calculate the segmentation error (SE). The segmentation results with a smallest SE were considered most accurate. Hence, image segmentation results were assessed with respect to specific geomorphological ‘feature types’, and segmentation parameters were optimized (Fig. 3).

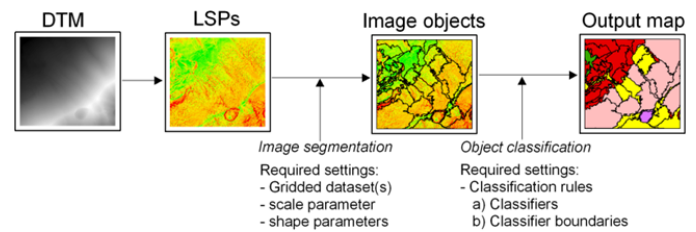


Figure 1. Flow diagram showing the OBIA steps and the required settings in the segmentation and classification procedures.

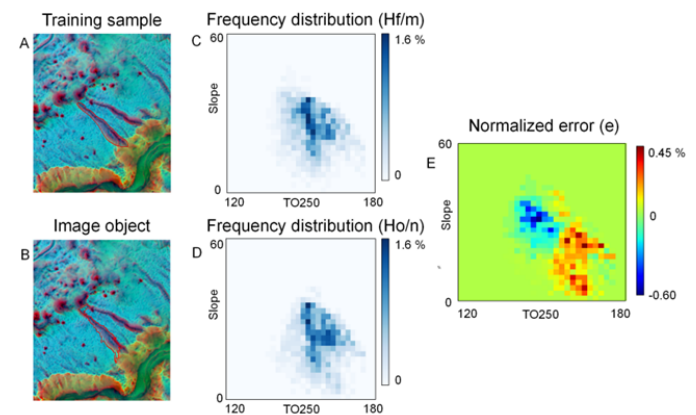


Figure 2. (A) An RGB composite was used to create training samples of geomorphological features. (B) Image objects were created in the same area of the training sample. (C-D) 2D frequency distribution matrices of training samples and image objects were calculated. (E) The difference between both frequency distribution matrices was used to calculate a normalized error.

**F. Classification optimization**

Based on the optimal segmentation parameters, image objects were created to extract a specific geomorphological ‘feature type’. From this feature type, three classifiers were selected that contain characteristic information about the feature, such as ‘distance to river’, ‘mean relative elevation’ and ‘mean slope angle’ as classifiers for extracting ‘river terraces.’

Classification results were iteratively assessed with a varying range of classifier values, where classification scores were calculated as a mean of user’s and producer’s accuracy [3]. In the first iteration the classifier values are set relatively wide (e.g. ‘mean slope angle’ of 0°–90°). Image objects are then classified based on various intervals with half the range of initial classifier values. Then, the interval values increase systematically in five steps towards the maximum classifier value.

For example, when the initial ‘mean slope angle’ is defined between 0°–90°, image objects are classified with intervals of a ‘mean slope angle’ of 0°–45°, 11.25°–56.25°, 22.5°–67.5°, 33.75°–78.75°, and 45°–90°. When the highest classification score is found within e.g. the interval of 0°–45°, iteration 2 will be restricted to 0°–45° and smaller intervals will be used (i.e. 0°–22.5°, 5.63°–28.13°, 11.25°–33.75°, 16.88°–39.38°, and 22.5°–45°). The iterative process continues while classification scores increase and interval values decrease.

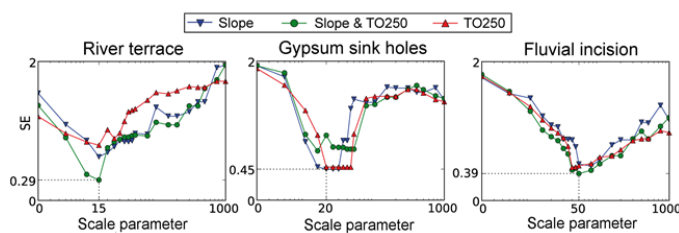


Figure 3. Segmentation errors (SE) are plotted against the scale parameter. The segmentation parameters corresponding to the smallest error were considered best for creating image objects for the specific geomorphological ‘feature type’.

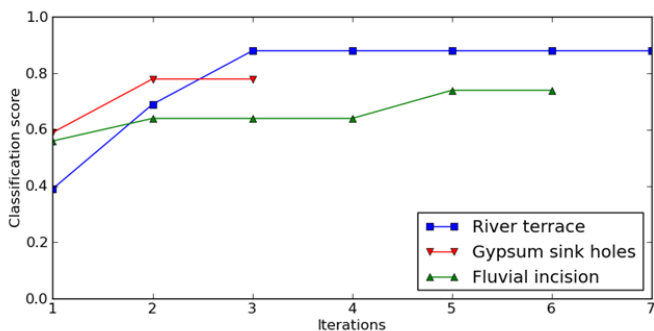


Figure 4. The maximum classification scores plotted against the iterations per geomorphological ‘feature type’. The optimization procedure stopped when classification scores no longer increased when interval values decreased.

**G. Stratified feature extraction**

Each ‘feature type’ was optimized and extracted individually and in a stratified way. This means that first the entire area was segmented based on segmentation parameters of the first feature of interest. Then the ‘feature type’ was extracted based on optimized classification rules. The unclassified objects were then merged and resegmented based on optimized segmentation parameters of the subsequent ‘feature type’ of interest. The sequence in which features are extracted was determined by the user. Trial and error showed best results when smaller features with distinct boundaries are extracted first, followed by larger features with more fuzzy boundaries.

**III. RESULTS AND DISCUSSION**

**A. Segmentation parametrization**

The segmentation parametrization showed different optimal segmentation parameters for the different geomorphological ‘feature types’ (Fig. 3). A scale parameter of 15, 20, and 50 produced the smallest segmentation error (0.29, 0.45, and 0.39) for ‘river terrace’, ‘gypsum sink holes’ and ‘fluvial incision by the river Gamp’, respectively. ‘River terrace’ and ‘fluvial incision’ features were most accurately segmented with LSPs ‘Slope and TO250’. ‘Gypsum sink holes’ received the best segmentation score based on ‘Slope’ or ‘TO250’ only (equally good). However, visual inspection showed that the segmentation based on ‘TO250’ performed slightly better.

The absolute segmentation error values differed between the feature types. This means that image objects for ‘river terrace’ features were more accurately segmented than those of ‘fluvial incision’—with respect to the manually digitized training samples. In order to improve the segmentation including other LSPs for segmenting image objects may be necessary. In addition, variable segmentation parameters mean that multiple segmentations are necessary when analyzing multiple features. A stratified or multi-scale feature extraction approach is therefore necessary when classifying entire landscapes.

**B. Classification optimization**

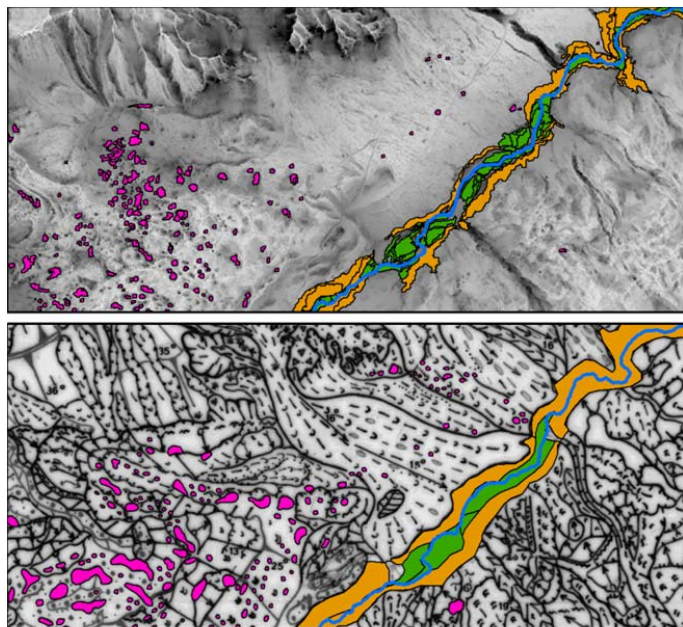
Fig. 4 shows a rapid increase in the classification score after few iterations in the optimization procedure. The best classification scores were 0.88, 0.78 and 0.74 for ‘river terrace’, ‘gypsum sink holes’, and ‘fluvial incision by the river Gamp’, respectively. These classification scores do not directly reflect the segmentation scores. For example ‘fluvial incision’ received a small segmentation error but a relatively low classification score. Different classifiers are likely necessary to improve classification results for these features.

Fig. 5 shows a subset of the output map; the best classification scores and the according classifier values are summarized in the feature signature library (Table 1). The large range of TO250

values for classifying ‘gypsum sink holes’ indicates that TO250 is likely not an accurate classifier for the specific feature type; a different classifier may produce better classification results. In addition, it may be possible to improve the classification accuracy by increasing the number of variables in the classification optimization procedure. Future research is planned to incorporate the remaining geomorphological feature types to create a full-covered geomorphological map of the area.

IV. CONCLUSIONS

We have presented a new method for the semi-automated optimization of object-based classification rules. Our results show that through optimization, a limited number of classifiers can be used for accurately classifying geomorphological features in complex terrain. By using segmentation and classification optimization we can more objectively apply OBIA for analyzing high-resolution datasets. Classification schemes can now be standardized for automated and effective data analysis. In addition, by automating mapping procedures, this research increases the efficiency of geomorphological research.



**Legend**  
 River (blue line) River terrace (green square) Fluvial incision (orange square) Gypsum sink hole (magenta square)

Figure 5. The upper figure shows a subset of the produced map showing the classified geomorphological features. In the background the TO250 LSP is visualized in black (low openness values) and white (high openness values). The lower figure shows a manual digitization of features based on the field map of [4] for visual comparison with the automated classification.

TABLE I. FEATURE SIGNATURE LIBRARY AND BEST CLASSIFICATION SCORES PER GEOMORPHOLOGICAL FEATURE TYPE

Feature signature library	Parameter/criteria	Geomorphological feature types		
		River terrace	Gypsum sink holes	Fluvial incision by river Gamp
Segmentation	Segmentation criteria	Slope, TO250	TO250	Slope, TO250
	Scale parameter	15	20	50
Classification	Mean slope [°]	3 – 14	23 – 68	> 25
	Mean TO250 [°]	-	90 – 210	< 150
	Mean REL250 [%]	3 – 16	-	-
	Distance to river [m]	< 47	-	< 63
	Mean filled area [m]	-	> 0.1	-
Classification scores	User’s accuracy	1.00	0.72	0.65
	Producer’s accuracy	0.76	0.85	0.83
	Classification score	0.88	0.78	0.74

ACKNOWLEDGMENT

This research is financially supported by the Research Foundation for Alpine and Subalpine Environments (RFASE) and the Virtual Lab for e-Science (vl-e) project. The ‘Land Vorarlberg’ has kindly allowed us to use their 1 m LiDAR DTM. We also thank ‘inatura, Naturerlebnis Dornbirn’ for their support.

REFERENCES

- [1] Anders, N.S., Seijmonsbergen, A.C., Bouten, W, in press. “Segmentation optimization and stratified object-based analysis for semi-automated geomorphological mapping”. Remote Sensing of Environment.
- [2] Baatz, M., Schäpe, A., 2000. “Multiresolution segmentation—an optimization approach for high quality multi-scale image segmentation.” In: Angewandte Geographische Informationsverarbeitung XII. Beiträge zum AGIT-Symposium Salzburg. Vol. 200. pp. 12–23.
- [3] Congalton, R., Green, K., 1999. “Assessing the accuracy of remotely sensed data: principles and practices”. Lewis Publishers, Boca Raton.
- [4] Seijmonsbergen, A.C., 1992. “Geomorphological evolution of an alpine area and its application to geotechnical and natural hazard appraisal”, PhD thesis, University of Amsterdam, 109 pp.
- [5] Van Asselen, S., Seijmonsbergen, A. C., 2006. “Expert-driven semi-automated geomorphological mapping for a mountainous area using a laser DTM”. Geomorphology 78 (3-4), 309 – 320.
- [6] Yokoyama, R., Shirasawa, M., Pike, R. J., 2002. “Visualizing topography by openness: a new application of image processing to digital elevation models”. Photogrammetric engineering and remote sensing 68, 257–265.